A novel 7-hypoxia-related long non-coding RNA signature associated with prognosis and proliferation in melanoma

YI LUO[1], TINGHAO LI[2], HENGGUANG ZHAO[3] and AIJUN CHEN[1]

Departments of [1]Dermatology and [2]Urology, The First Affiliated Hospital of Chongqing Medical University, Chongqing 400016; [3]Department of Dermatology, The Second Affiliated Hospital of Chongqing Medical University, Chongqing 400010, P.R. China

Received February 16, 2022; Accepted May 12, 2022

DOI: 10.3892/mmr.2022.12771

Abstract. Hypoxia-related long non-coding RNAs (lncRNAs) are important indicators of the poor prognosis of cancers. The present study aimed to explore the potential relationship between melanoma and hypoxia-related lncRNAs. The transcriptome and clinical data of patients with melanoma were downloaded from The Cancer Genome Atlas database. The prognostic hypoxia-related lncRNAs were screened out using Pearson's correlation test and univariate Cox analysis. As a result, a hypoxia-related-lncRNA signature based on the expression of 7 lncRNAs was constructed, with one unfavourable [MIR205 host gene (MIR205HG)] and six favourable (T cell receptor β variable 11-2, HLA-DQB1 antisense RNA 1, AL365361.1, AC004847.1, ubiquitin specific peptidase 30 antisense RNA 1 and AC022706.1) lncRNAs as prognostic factors for melanoma. Patients with melanoma were divided into high- and low-risk groups based on the risk score obtained. Survival analyses were performed to assess the prognostic value of the present risk model. Potential tumour-associated biological pathways associated with the present signature were explored using gene set enrichment analysis. The CIBERSORT algorithm demonstrated the important role of the hypoxia-related lncRNAs in regulating tumour-infiltrating immune cells. Clinical samples collected from our center partly confirmed our findings. Cell Counting Kit-8 and flow cytometry assays indicated the suppression of proliferation of melanoma cells following inhibition of MIR205HG expression. Indicators of the canonical Wnt/β-catenin signalling pathway were detected by western blotting. The present study demonstrated that MIR205HG could promote melanoma cell proliferation partly via the canonical Wnt/β-catenin signalling pathway. These findings indicated a 7-hypoxia-related-lncRNA signature that can serve as a novel predictor of melanoma prognosis.

Correspondence to: Dr Aijun Chen, Department of Dermatology, The First Affiliated Hospital of Chongqing Medical University, 1 Youyi Road, Yuzhong, Chongqing 400016, P.R. China
E-mail: chenaijunhx@126.com

Key words: hypoxia, melanoma, long non-coding RNA, MIR205 host gene, proliferation

Introduction

Melanoma is the 19th most common cancer diagnosis worldwide, representing <5% of skin cancers and accounting for 80% of skin cancer-related deaths (1). Compared with other cancer types, the global incidence of cutaneous melanoma has been increasing annually at a more rapid rate (2). Every year, ~160,000 new cases of invasive melanoma and 48,000 deaths due to the disease are recorded worldwide (3). The oncogenesis and developmental mechanisms of melanoma remain unclear and require further exploration. Furthermore, it is of vital importance to explore efficient biomarkers for early and accurate diagnosis.

Tumorigenesis and malignancy development are complex processes affected by various factors. Due to genetic changes and epigenetic defects, the tumour microenvironment, which consists of cellular and non-cellular components, also serves an important regulatory role in cancer progression (4). Tumour hypoxia is a condition wherein solid tumours have lesser oxygenation than that observed in normal tissues (5), which results in the obstruction of therapy and the progression of malignancy (6). Various studies have demonstrated the crucial role of hypoxia in the malignant behaviour of melanoma cells, including abnormal proliferation, distant metastasis and immune evasion (7-9). As a type of RNA that does not encode proteins and has a length >200 nucleotides, long non-coding RNAs (lncRNAs) have been explored in the occurrence and development of numerous tumours (10,11). lncRNAs participate in the modification of proteins that affect the survival and proliferation of cancer cells and thereby serve a role in cancer cell survival and development, even in hypoxic circumstances (12). It has been reported that hypoxia yield proliferation-associated lncRNA acts as a competing endogenous RNA (ceRNA) that binds to microRNA (miRNA/miR)-431-5p under hypoxic conditions to upregulate CDK14 expression, resulting in gastric cancer cell proliferation (13). In colorectal cancer cells, lncRNA COL4A2 antisense RNA 1 facilitates growth and glycolysis under hypoxia via the miR-20b-5p/hypoxia-inducible factor 1α subunit axis (14). Several studies have also explored the

relationship between malignant melanoma progression and hypoxia-related lncRNAs, including long intergenic non-protein coding RNA 518 and non-coding RNA activated by DNA damage (15,16). Therefore, lncRNAs may serve a crucial role in hypoxia-related malignancy development and poor melanoma prognosis.

lncRNA-based signatures have recently drawn attention due to their high predictive accuracy (17,18). However, hypoxia-related lncRNAs as biomarkers for prognostic prediction in melanoma are yet to be investigated. The present study aimed to build a hypoxia-related-lncRNA signature and nomogram that can improve the overall survival (OS) predictability in patients with melanoma using bioinformatics. The present study identified a 7-hypoxia-related-lncRNA signature through a comprehensive analysis of The Cancer Genome Atlas (TCGA) database and two hypoxia-related gene sets. The present signature was verified and analysed by combining the clinical features of melanoma, and validated using clinical samples and *in vitro* experiments.

Materials and methods

Data collection. The transcriptome expression profiles corrected by FPKM (fragments per kilobase of exon per million mapped fragments) and clinical information were downloaded from TCGA database (https://portal.gdc.cancer.gov). The details of the clinical characteristics, including OS, survival time, age, sex, stage, tumour size, distant metastasis and lymph node metastasis, of the included cohort of 471 patients are listed in Table SI. Among these 494 patients, 23 patients with incomplete data or vague living status were excluded from the present study. The hypoxia-related gene expression profiles KRIEG and WINTER were downloaded from the Gene Set Enrichment Analysis (GSEA) database (http://www.gsea-msigdb.org) and are listed in Table SII. The data used in the present study were downloaded on May 21, 2021.

Establishment of a hypoxia-related-lncRNA signature as a prognostic model. Pearson's correlation analysis was used to identify hypoxia-related lncRNAs. The correlation between lncRNA expression and hypoxia-related gene expression was calculated. The selection criteria included values with $|R^2|>0.7$ and $P<0.001$. Univariate Cox regression analysis was used to screen for prognosis-associated hypoxia-related lncRNAs. A hazard ratio (HR) <1 represented favourable OS outcomes, and a HR >1 represented poor OS outcomes. lncRNAs with $P<0.05$ were selected as hypoxia-related lncRNAs and used to construct the present prognostic model.

Evaluation of the hypoxia-related-lncRNA prognostic signature. Multivariate Cox regression analysis was used to create a signature, and the risk score formula was as follows: $(\text{RiskScore}) = \sum_{i=1}^{n}(\text{Expi} * \text{Coei})$. In the aforementioned formula, 'n' indicates the number of prognostic genes, 'Expi' indicates the level of lncRNA I expression, and 'Coei' indicates the regression coefficient of the corresponding lncRNA obtained using the multivariate Cox regression model. Patients with melanoma were divided into high- and low-risk subgroups according to the median risk score. A survival curve was used to compare the OS of patients between the high- and low-risk groups. The diagnostic efficacy and clinicopathological characteristics of the 7-hypoxia-related-lncRNA signature were evaluated using receiver operating characteristic (ROC) curves. The risk score efficiency of the present signature to independently predict the survival rate was assessed using univariate and multivariate Cox regression analyses.

Estimation of clinical independence and construction of the nomogram. The 'rms' R package was used to integrate the clinical features with the risk scores obtained. The present 7-hypoxia-related-lncRNA signature was used to construct a nomogram for further clinical prediction. Variates of clinical features were categorized into dichotomous variables and defined by Cox regression analysis. Samples with incomplete clinical information were excluded to make the results consistent. A horizontal straight line was drawn to ascertain the points for each variable by variables feature. Subsequently, the total points of each patient were calculated by adding the points for all variables together, followed by normalization to a distribution of 0 to 100. The performance of the present nomogram was evaluated using calibration plots and time-dependent ROC curves.

Principal component analysis (PCA). PCA was conducted using the 'scatterplot3D' R package to illustrate the level of expression of melanoma samples in the low- and high-risk groups. Patients were divided into different subgroups using different gene sets, including the present 7-hypoxia-related-lncRNA gene set, hypoxia-related-lncRNA gene set, hypoxia-related gene set and whole gene sets.

Construction of the co-expression network. The lncRNA-miRNA-mRNA co-expression network was constructed using Cytoscape (version 3.8.2) to elucidate the association of the hypoxia-related lncRNAs with their target miRNAs and downstream mRNAs. The lncRNA-miRNA connection was predicted using data downloaded from miRcode (http://www.mircode.org). TargetScan (version 8.0) (https://www.targetscan.org), miRDB (http://www.mirdb.org) and miRTarBase databases (http://mirtarbase.mbc.nctu.edu.tw/php/index.php) were used to screen for miRNAs and their corresponding target mRNAs. The selected mRNAs were compared with hypoxia-related mRNAs to obtain reliable hypoxia-related lncRNAs.

GSEA. GSEA was employed to identify enriched gene sets in the high-risk groups. The Gene Ontology-Biological Process (GO-BP) ontology gene sets (c5.go.bp.v7.4.symbols.gmt) were downloaded from the Molecular Signatures Database (http://www.gsea-msigdb.org). Gene set permutations were performed 1,000 times for each analysis.

Immune cell infiltration analysis. The CIBERSORT algorithm of the R software was used to determine the profile of tumour-infiltrating immune cells (TIICs; including 22 immune cells) in all tumour samples. The relationship between TIICs and risk scores was analysed using the limma package. Comparisons of the TIIC levels between the high- and low-risk groups were estimated using the unpaired Student's t test.

Table I. Sequences of small interfering RNAs and primer sequences for reverse transcription-quantitative PCR.

Designation	Gene/siRNA	Sequences (5'-3')	Organism
Primer	HLA-DQB1-AS1	F: AGCAGAGTCCAGGGTGTATTG	*Homo sapiens*
		R: GCTGCTAGTGGTCGGGAAG	
	TRBV11-2	F: GTGACCCTGATTGGGCAAAG	
		R: TATCTGGGAGACTGGGCAAC	
	MIR205HG	F: AGGAGTCATTTCTGTTCCGCA	
		R: CAAATAGTGTCCCAGCCACCT	
	GAPDH	F: CAGTGGCAAAGTGGAGATTGTTG	
		R: TCGCTCCTGGAAGATGGTGAT	
siRNA	MIR205HG-siRNA-1	F: UCUCCUUCAAUUCCACUUUTT	*Homo sapiens*
		R: AAAGUGGAAUUGAAGGAGATT	
	MIR205HG-siRNA-2	F: GAGACAGCCAGAGAGAAAUTT	
		R: AUUUCUCUCUGGCUGUCUCTT	

F, forward; HLA-DQB1-AS1, HLA-DQB1 antisense RNA 1; MIR205HG, MIR205 host gene; R, reverse; siRNA, small interfering RNA; TRBV11-2, T cell receptor β variable 11-2.

Cell culture. A375 human melanoma cells were purchased from the Institute of Biochemistry and Cell Biology of the Chinese Academy of Sciences. Cells were incubated in DMEM (Gibco; Thermo Fisher Scientific, Inc.) supplemented with 10% FBS (Gibco; Thermo Fisher Scientific, Inc.). The cells were seeded in cell culture plates and cultivated in a humidified incubator at 37˚C with 5% CO_2.

Human tissue specimens. The human melanoma specimens were provided by the Department of Dermatology of the Chongqing Medical University (Chongqing, China) from October 2021 to March 2022. The present study was performed using 20 melanoma samples and their paired adjacent tissues, which were collected from 10 males and 10 females, with age range from 49 to 58 years old. Inclusion criteria were as follows: People who were diagnosed with melanoma by pathological examination at first time with medical history which was detailed enough to meet the statistical needs of this trial. Exclusion criteria were as follows: People who were diagnosed as melanoma or treated previously; people with other special conditions (such as severe chronic secondary fungi or bacterial infection); and people with metastatic melanoma. The expression levels of three lncRNAs were detected using reverse transcription-quantitative PCR (RT-qPCR). The present study was approved (approval no. 2021-487) by the Institute Research Ethics Committee of the First Affiliated Hospital of Chongqing Medical University (Chongqing, China). All individuals provided written informed consent for the use of their samples for clinical research.

Small interfering RNA (siRNA/si) interference assay. All siRNAs targeting human MIR205 host gene (MIR205HG, Gene ID: 642587; si-MIR205HG-1 and si-MIR205HG-2) and scrambled negative control (si-NC) were designed and synthesized by Shanghai GenePharma Co., Ltd. and are listed in Table I. The siRNAs were transfected into A375 cells using Lipofectamine® 2000 (Invitrogen; Thermo Fisher Scientific, Inc.) according to the manufacturer's protocol. In brief, A375 cells were seeded into 6-well plates at a density of $1.2x10^5$ cells per well and routinely cultured until the confluence reached 70%. Then the medium was changed to 2 ml DMEM without serum, supplemented with 5 μl Lipofectamine® 2000 and 5 μl (20 μM) siRNA to transfect for 6 h at 37˚C with 5% CO_2. Subsequent experimentation was performed 48 h after transfection. The efficiency of MIR205HG knockdown was verified using RT-qPCR.

RT-qPCR. Total RNA was extracted from the two groups using TRIzol® reagent (Takara Bio, Inc.) according to the manufacturer's protocol. First-strand cDNA synthesis was performed using the PrimeScript RT reagent kit (Takara Bio, Inc.). The following thermocycling conditions were used for RT: 25˚C for 5 min, 42˚C for 40 min and 85˚C for 2 min. Subsequently, qPCR was performed using an ABI7500 real-time PCR system using SYBR green (Takara Bio, Inc.). The qPCR thermocycling conditions were as follows: 94˚C for 2 min, followed by 40 cycles of 94˚C for 30 sec and 55˚C for 45 sec. All RT-qPCR primers were purchased from Shanghai GenePharma Co., Ltd. and the sequences are listed in Table I. Each sample was detected at least three times independently. The $2^{-\Delta\Delta Cq}$ method was utilized to quantify the expression levels (19).

Cell proliferation assay. The growth rate of A375 cells was assessed using a Cell Counting Kit-8 assay (CCK-8; Boster Biological Technology). A375 cells transfected with different siRNAs were seeded into 96-well plates (5,000 cells per well). After incubation for 48 h at 37˚C with 5% CO_2, 10 μl CCK-8 reagent was added to each well. The absorbance of the cell medium at 450 nm was recorded to assess the cell viability in each group.

Cell cycle analysis. A375 cells cultured in six-well plates were transfected with different siRNAs. After transfection for 48 h, cells were collected and fixed with 70% cooling ethanol at 4˚C

overnight. Following staining with propidium iodide solution containing RNase A, cells were washed with PBS three times. After an incubation of 30 min at room temperature, the cell cycle distribution was analysed using a FACSCalibur flow cytometer (BD Accuri C6 Plus). CytExpert software (version 2.4.0.28; Beckman Coulter, Inc.) was employed for analysis.

Western blotting. Total protein was extracted using RIPA lysis buffer (Beyotime Institute of Biotechnology) containing 1% PMSF and 1 mmol/l β-glycerophosphate sodium salt hydrate, which were both purchased from Selleck Chemicals. The protein concentration was calculated using a BCA protein quantitative kit (Beyotime Institute of Biotechnology). A 10% SDS-polyacrylamide gel (Beyotime Institute of Biotechnology) was used to separate the same amount of protein sample (20 μg) and protein was transferred to nitrocellulose membranes (MilliporeSigma). Membranes were blocked with 5% skim milk in Tris-buffered saline containing 1% Tween 20 for 2 h at room temperature. Membranes were incubated overnight at 4˚C with the following primary antibodies: Anti-phospho-GSK3-β (1:1,000; cat. no. 5558; Cell Signaling Technology, Inc.), anti-GAPDH (1:10,000; cat. no. 10494-1-AP; ProteinTech Group, Inc.), anti-c-Myc (1:1,000; cat. no. A5011; Bimake), anti-β-catenin (1:1,000; cat. no. 8480; Cell Signaling Technology, Inc.), anti-phospho-β-catenin (1:1,000; cat. no. 4176; Cell Signaling Technology, Inc.), anti-GSK3-β (1:1,000; cat. no. 121456; Cell Signaling Technology, Inc.). Following primary incubation, membranes were incubated with HRP-labeled Goat Anti-Rabbit IgG (H+L) (1:1,000; cat. no. A0208; Beyotime Institute of Biotechnology) at room temperature for 2 h. Subsequently, enhanced chemiluminescence reagents (MilliporeSigma) were employed to assess protein expression and protein expression was normalized to that of GAPDH. The blots were quantified using Evolution (version 18.0.8.0, Viber Lourmat).

Statistical analysis. The R software (version 3.5.1) with corresponding packages and GraphPad Prism 7 (GraphPad Software, Inc.) were used for statistical analyses. Unless specified otherwise above, $P<0.05$ was considered to indicate a statistically significant difference. The PERL programming language (version 5.30.2; http://www.perl.org) was employed to process data. The Kaplan-Meier method and log rank test were performed to compare the OS between the high- and low-risk groups. The results of analyses were presented as the mean ± standard deviation. The Student's t-test was utilized to analyze the differences between two groups according to the specific. Dunnett's test was the post hoc test used following one-way ANOVA to compare three or more groups.

Results

Construction of the hypoxia-related-lncRNA signature. RNA expression data from 471 patients with melanoma and 1 normal adjacent tissue were extracted, and two hypoxia-related gene sets (KRIEG and WINTER) were selected to identify hypoxia-related oncogenes. A total of 882 hypoxia-related mRNAs were acquired (Fig. 1A). Using Pearson's correlation analysis between the lncRNA samples from 471 patients with melanoma and hypoxia-related genes, 72 hypoxia-related lncRNAs were identified. The selection criteria were $|R^2|>0.7$ and $P<0.001$. Univariate Cox regression analysis was then performed to analyse the 72 lncRNAs. The survival data revealed that 23 hypoxia-related-lncRNAs were independent prognostic factors in patients with melanoma. To eliminate the mutual influence among lncRNAs, multivariate Cox regression analysis was used (Fig. 1B). Finally, a hypoxia-related-lncRNA signature that included 7 lncRNAs was constructed, with one unfavourable (MIR205HG) and six favourable [T cell receptor β variable 11-2 (TRBV11-2), HLA-DQB1 antisense RNA 1 (HLA-DQB1-AS1), AL365361.1, AC004847.1, ubiquitin specific peptidase 30 (USP30) antisense RNA 1 (USP30-AS1) and AC022706.1] lncRNAs as prognostic factors for melanoma (Fig. 1C; Table II).

Using the present 7-hypoxia-related-lncRNA signature, patients with melanoma were classified into two groups based on their risk scores (Fig. 1D). The OS time and survival rate were longer and higher, respectively, in the low-risk group compared with the high-risk group (survival rate, 62.33% in the low-risk group vs. 44.84% in the high-risk group; Fig. 1E), which was also demonstrated in survival analysis ($P<0.001$; Fig. 1F). The diagnostic efficacy of the signature was estimated using time-dependent ROC curves, wherein the area under the curve (AUC) was >0.7 for both 1 and 5 years (Fig. 1G). To validate the reliability and stability of the present risk model, the training cohort was divided into two sub-validation cohorts (n=314 in sub-validation cohort 1 and n=132 in sub-validation cohort 2) at random. Kaplan-Meier survival analysis revealed a worse prognosis in high-risk group patients in both cohorts ($P<0.001$ and $P<0.001$; Fig. 1H and J). Time-dependent ROC curves showed promising accuracy of the present risk model, particularly at 5 years in both sub-validation cohort 1 (AUC=0.706) and sub-validation cohort 2 (AUC=0.732) (Fig. 1I and K). These results suggested that the present signature could predict the survival period of patients with melanoma.

Association of the hypoxia-related-lncRNA signature with the clinicopathological features of melanoma. The association between the risk scores and clinicopathological features was assessed. The results suggested that the 7-hypoxia-related-lncRNA signature was closely related to melanoma progression. Specifically, patients with American Joint Committee on Cancer (AJCC) stage III-IV, T stage 3-4 and N stage ≥1 had higher risk scores than patients with AJCC stage I-II ($P=0.0246$), T stage 0-2 ($P<0.001$) and N stage <1 ($P=0.0104$) (Fig. 2C, E and F). However, differences in age, sex and M stage were not observed ($P>0.05$; Fig. 2A, B and D). The results indicated that the present 7-hypoxia-related-lncRNA signature was closely related to the progression of melanoma.

Independent risk characteristics for the hypoxia-related-lncRNA signature. The prognostic ability of the 7-hypoxia-related-lncRNA signature in patients with melanoma was assessed via univariate and multivariate Cox regression analyses. The results demonstrated that the risk score of the present signature [HR, 1.694; 95% confidence interval (95% CI), 1.396-2.056; $P<0.001$], age (HR, 1.015; 95% CI, 1.004-1.026; $P=0.008$), T stage (HR, 1.283; 95% CI, 1.081-1.522; $P=0.004$) and N stage (HR, 1.587; 95% CI,

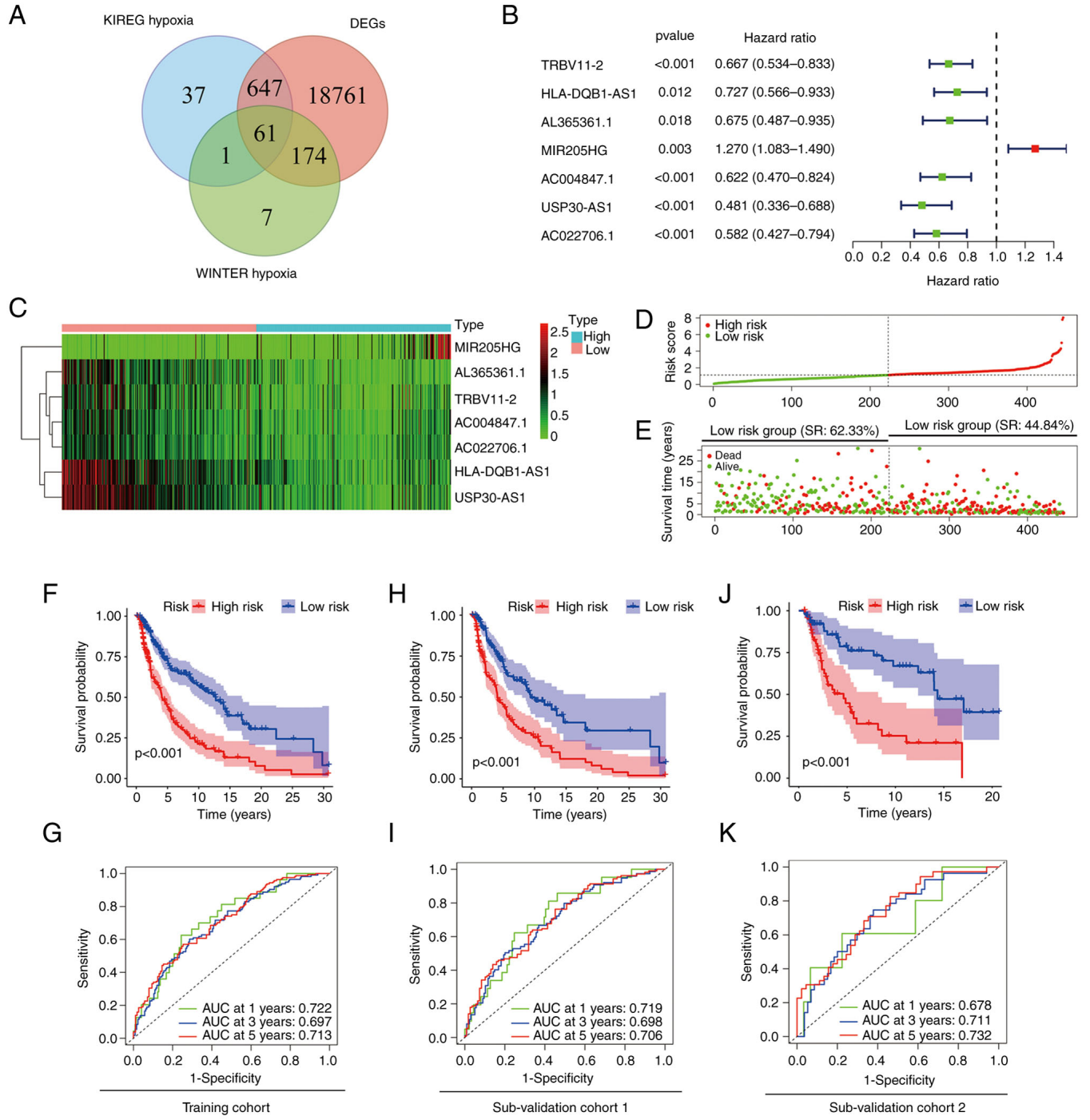

Figure 1. Construction of the hypoxia-related-lncRNA signature. (A) Overlap between two hypoxia-related gene sets (KRIEG and WINTER) and mRNA expression levels in melanoma. (B) Multivariate Cox regression analysis was used to identify hypoxia-related lncRNAs. (C) Heatmap demonstrating hypoxia-related-lncRNA signature expression in patients. (D) Patients sorted into high- and low-risk groups according to the median risk score. (E) Survival status and survival time of each patient. The SR was calculated in both the high- and low-risk group. (F) Survival curve analysis of the 7-hypoxia-related-lncRNA signature in training cohort. (G) Time-dependent ROC curve analysis in training cohort. (H) Survival curve of the 7-hypoxia-related-lncRNA signature in sub-validation cohort 1. (I) Time-dependent ROC curves analysis in sub-validation cohort 1. (J) Survival curve of the 7-hypoxia-related-lncRNA signature in sub-validation cohort 2. (K) Time-dependent ROC curves analysis in sub-validation cohort 2. lncRNA, long non-coding RNA; ROC, receiver operating characteristic; SR, survival rate.

1.245-2.024; P<0.001) were significantly related to the OS of patients with melanoma as independent prognostic indicators (Fig. 3A and B). The time-dependent ROC curve also revealed a 0.789 AUC value of the risk score, indicating appropriate sensitivity and specificity of the present 7-hypoxia-related-lncRNA signature in predicting the survival of patients with melanoma compared with other clinicopathological parameters (Fig. 3C).

Stratification analysis of clinical features using the hypoxia-related-lncRNA signature. A stratified analysis of patients with melanoma based on clinical features, including sex, age, AJCC stage and TNM stages, was performed. The Kaplan-Meier survival curve analysis illustrated that patients with melanoma had higher hypoxia-related-lncRNA signature-predicted risk scores and a shorter OS period compared

Table II. Hypoxia-related long non-coding RNAs associated with the overall survival of patients with melanoma.

Gene symbol	Aliases	Ensemble ID	Location	P-value	HR
TRBV11-2	Lnc-MGAM2-1	ENSG00000241657	chr7:142,433,895-142,434,394	0.000361432	1.330058039
HLA-DQB1-AS1	HSALNG0049432	ENSG00000223534	chr6:32,659,879-32,660,729	0.012388052	0.726654702
AL365361.1	lnc-KCNA3-3	ENSG00000259834	chr1:110653560-110657040	0.018247458	0.675041646
MIR205HG	NPC-A-5	ENSG00000230937	chr1:209,425,755-209,433,438	0.003259287	1.270371188
AC004847.1	Lnc-MYO1G-1	ENSG00000260997	chr7:44,958,998-44,960,909	0.032147891	1.76373733
USP30-AS1	HSALNG0093872	ENSG00000256262	chr12:109,051,790-109,054,033	0.0000617	0.481152446
AC022706.1	Lnc-SLFN5-1	ENSG00000267364	chr17:33,640,521-33,651,919	0.000622238	1.508349735

HLA-DQB1-AS1, HLA-DQB1 antisense RNA 1; HR, hazard ratio; MIR205HG, MIR205 host gene; TRBV11-2, T cell receptor β variable 11-2; USP30-AS1, USP30 antisense RNA 1.

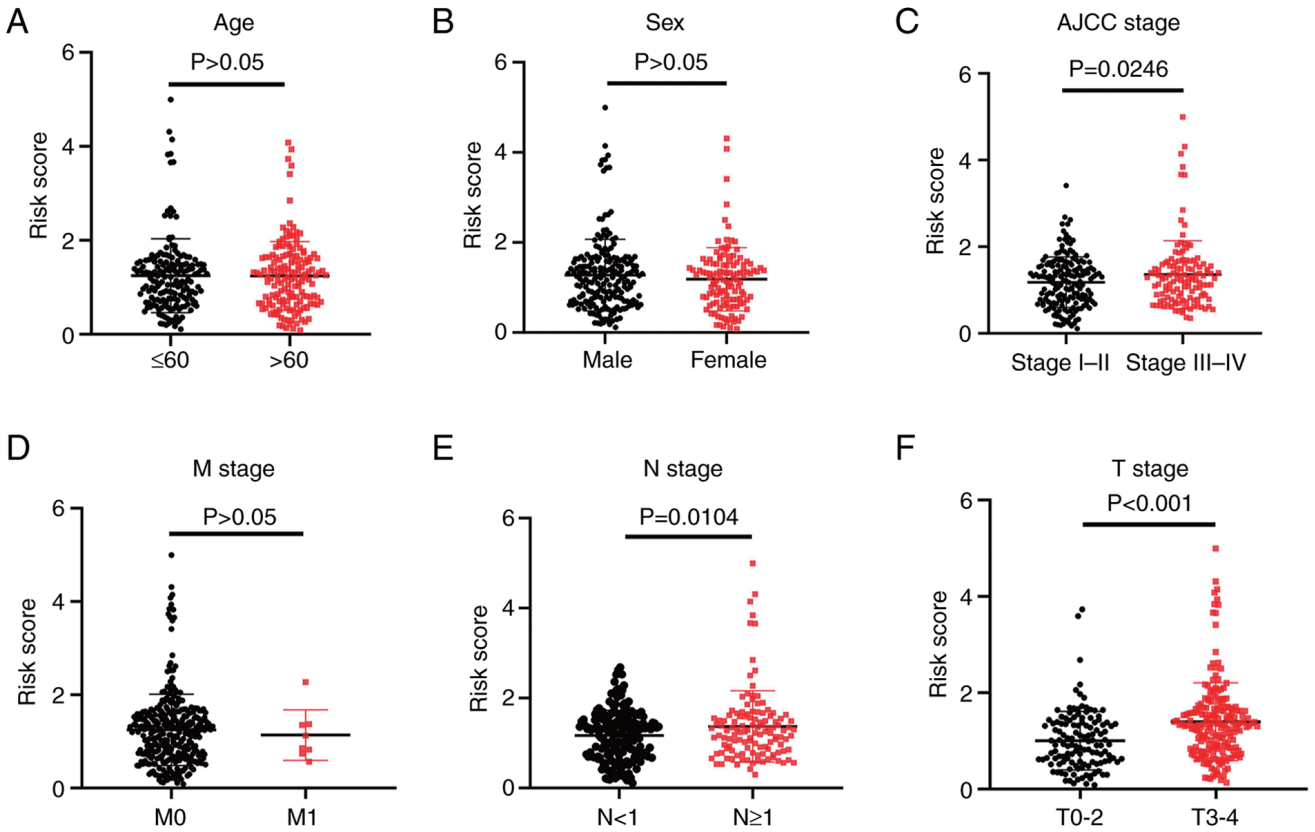

Figure 2. Association of the 7-hypoxia-related-long non-coding RNA signature with clinicopathological features in melanoma. Association between the signature risk scores and the clinicopathological features, including (A) age (>65 vs. ≤65; unpaired Student's t-test, P=0.9469), (B) sex (female vs. male; unpaired Student's t-test, P=0.2866), (C) American Joint Committee on Cancer stage (stage I-II vs. stage III-IV; unpaired Student's t-test, P=0.0246), (D) M stage (stage 0 vs. stage 1; unpaired Student's t-test, P=0.6898), (E) N stage (stage <1 vs. stage ≥1; unpaired Student's t-test, P=0.0104) and (F) T stage (stage 0-2 vs. stage 3-4; unpaired Student's t-test, P<0.001).

with the low-risk groups for most clinical and clinicopathological features (Fig. S1A-K); however, the patients at the M1 stage (P=0.959) were an exception, probably due to the small sample size (Fig. S1L). These results indicated that the present 7-hypoxia-related-lncRNA signature could accurately predict the survival period of patients with melanoma.

PCA using the hypoxia-related-lncRNA signatures. PCA was employed to detect the different distribution patterns between the low- and high-risk groups of patients with melanoma. The 7-hypoxia-related-lncRNA gene set (Fig. 4A) was used to create a low- and high-risk group. A significant separation of the risk score based on the hypoxia-related lncRNA gene set (Fig. 4B), hypoxia-related gene set (Fig. 4C) and all gene sets (Fig. 4D) was not observed, indicating that, compared with other distribution patterns, the present 7-hypoxia-related-lncRNA signature could accurately divide patients with melanoma into risk groups.

Establishment and validation of the nomogram. To diagnose or predict the onset or progression of melanoma, a nomogram was

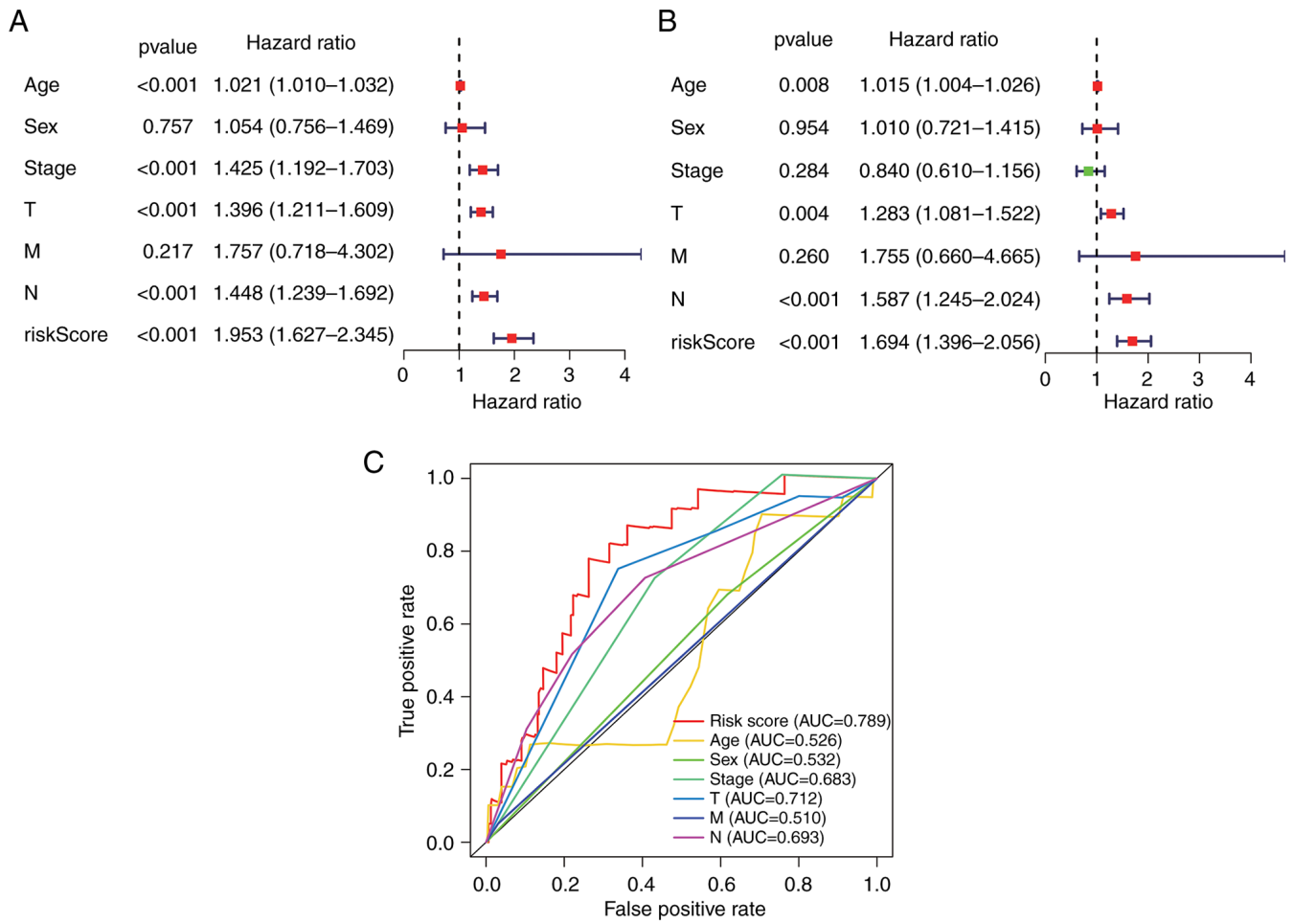

Figure 3. Hypoxia-related-lncRNA signature is an independent factor of prognostic indicators of melanoma. (A and B) Univariate and multivariate Cox regression analysis demonstrated the association between overall survival and clinicopathological parameters and the risk score. (C) Receiver operating characteristic curve analysis indicated the prognostic accuracy of clinicopathological parameters and the hypoxia-related lncRNA prognostic risk score. lncRNA, long non-coding RNA.

established based on the risk score and other clinical features, including age, AJCC stage, T stage and N stage (Fig. 5A). The calibration plots satisfactorily predicted the 3-year OS rate compared with the ideal model (Fig. 5B) but unsatisfactorily predicted the 5-year OS rate (Fig. 5C). Time-dependent ROC curves revealed that the AUC values of the nomogram at 3 and 5 years were 0.709 and 0.715, respectively (Fig. 5D).

Construction of the ceRNA network and GSEA. To explore the mechanism of the present 7-hypoxia-related-lncRNA signature, the 7 hypoxia-related lncRNAs and their corresponding miRNAs were first predicted using miRcode. The results indicated that 92 miRNAs could interact with lncRNA MIR205HG, lncRNA TRBV11-2 and lncRNA HLA-DQB1-AS1 (Table SIII). Additionally, the corresponding miRNA target proteins were predicted using three databases (TargetScan, miRDB and mieTarBase). Via comparison with the obtained hypoxia-related mRNAs, it was determined that the present signature targeted 17 miRNAs and 54 mRNAs, and a co-expression RNA network was constructed (Fig. 6A). To explore the relationship between the expression of the 7-hypoxia-related-lncRNA signature and melanoma classification, including biological processes involved in progression, GSEA was employed to identify key Gene Ontology terms and pathway enrichment analysis of high-risk score patients with melanoma in the GO-BP gene sets. Genes associated with a high-risk score were mainly enriched in the activation of immune response [normalized enrichment score (NES)=1.75; P=0.012], regulation of immune system process (NES=1.63; P=0.002), adaptive immune response (NES=2.05; P<0.001), development of immune system (NES=1.82; P<0.001), positive regulation of immune response (NES=1.94; P<0.001), positive regulation of cell death (NES=1.77; P=0.002), negative regulation of cell cycle (NES=1.57; P=0.028), positive regulation of Wnt signalling pathway (NES=1.85; P<0.001) and regulation of Wnt signalling pathway (NES=1.75; P=0.004) (Fig. 6B-K).

Regulation of TIICs by the 7-hypoxia-related lncRNAs. Based on the GSEA results in Fig. 6C-G, the present study explored the association between immune cell infiltration and the risk score. The CIBERSORT algorithm was used to validate the association of the hypoxia-related lncRNAs with TIICs in patients with melanoma. The proportion of TIICs in each patient with melanoma was investigated using the CIBERSORT algorithm (Fig. 7A). A comparison of the TIIC levels between the high- and low-risk groups showed an increased level of M0

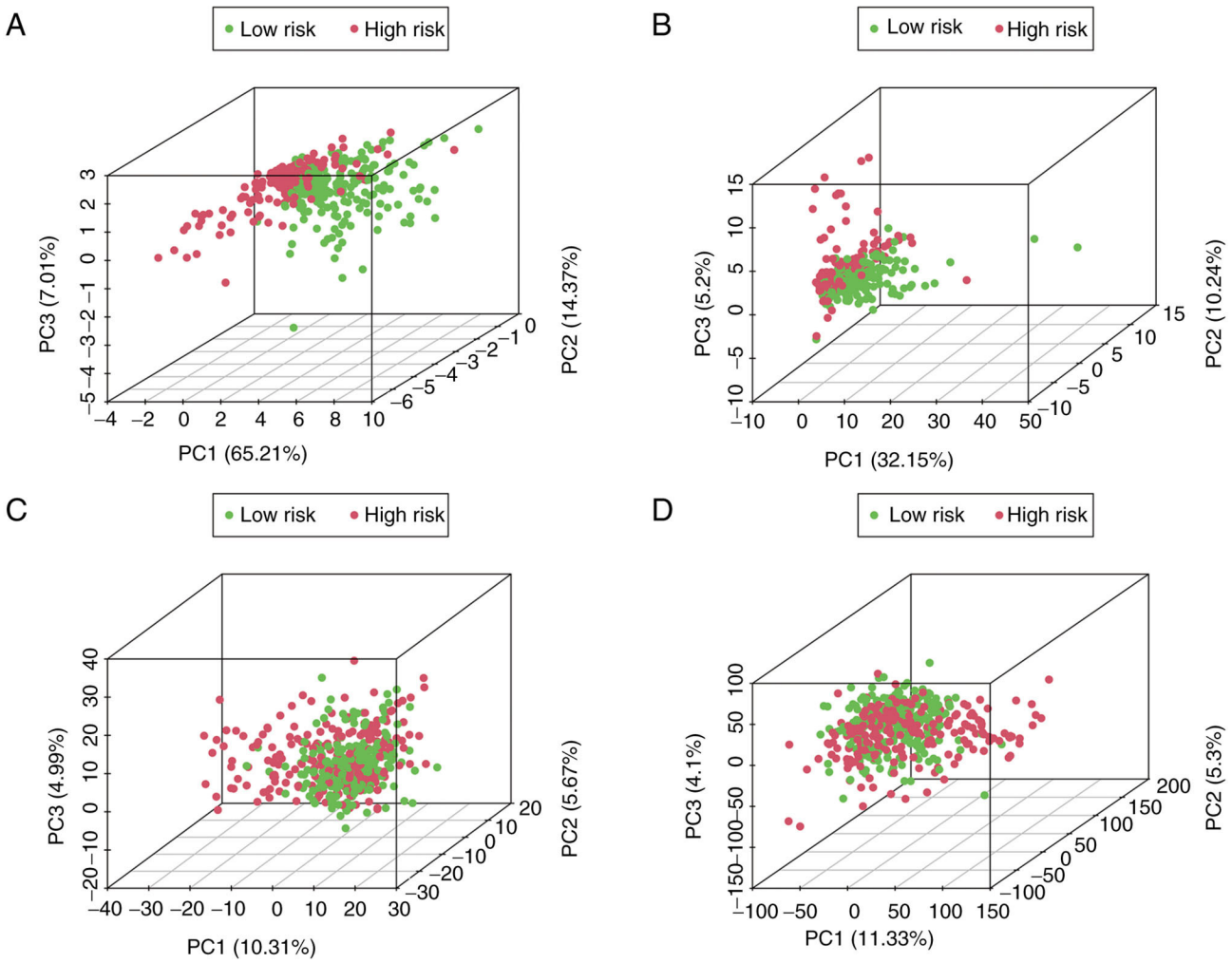

Figure 4. PCA. PCA between the high-risk group and the low-risk group based on (A) the hypoxia-related-lncRNA signature, (B) hypoxia-related lncRNAs, (C) hypoxia-related genes and (D) all gene sets. The red and green dots represent high- and low-risk genes, respectively. lncRNA, long non-coding RNA; PCA, principal component analysis.

macrophages (P<0.001) and resting mast cells (P=0.046) in the high-risk group, and a decreased number of plasma cells (P=0.002), $CD8^+$ T cells (P<0.001), resting memory $CD4^+$ T cells (P=0.036), activated memory $CD4^+$ T cells (P<0.001), follicular helper T cells (P<0.001), resting natural killer (NK) cells (P=0.007) and M1 macrophages (P<0.001) in the high-risk group (Fig. 7B). These results revealed the important role of the hypoxia-related lncRNAs in regulating TIICs.

MIR205HG silencing inhibits melanoma cell proliferation via the canonical Wnt/β-catenin signalling pathway. The expression levels of human leukocyte antigen (HLA), MIR205HG-1 and TRBV11 in melanoma and paired adjacent tissues of 20 clinical samples were detected using RT-qPCR. The expression levels of HLA and TRBV11 were elevated, whereas the expression levels of MIR205HG-1 were decreased in the normal tissues (Fig. 8A-C). These results suggested the specificity of siRNA to MIR205HG. To investigate the role of MIR205HG in melanoma cells, A375 cells were transfected with two sequences of siRNAs that target MIR205HG and negative control (NC) siRNA. As shown in Fig. 8D, the knockout efficiency was detected using RT-qPCR. Then si-MIR205HG-1 was selected for further experimentation since it significantly inhibited the expression of MIR205HG in A375 cells compared with the NC group. The results of cell cycle distribution analysis using flow cytometry indicated that the percentage of cells in the S-phase was greater in the siMIR205HG-1 group than in the NC group in A375 cells (Fig. 8E). Additionally, detection of cell viability using a CCK-8 assay also demonstrated the proliferation of A375 cells, which was inhibited to a greater extent compared with the NC group cells after si-MIR205HG-1 transfection (Fig. 8F). Based on the aforementioned GSEA results, the potential relationship between the MIR205HG and the Wnt/signaling pathway was investigated. Subsequently, the expression levels of relative proteins were detected by western blotting (Fig. 8G). The results revealed that the expression levels of p-β-catenin and p-GSK3-β in A375 cells were increased after siMIR205HG-1 transfection, while the expression of c-Myc and β-catenin was decreased. The ratio of phosphorylated protein to total protein (p/t, phosphorylated/total) was calculated. The results demonstrated that phosphorylation modification on GSK3-β was enhanced (p/t, NC. vs. si-MIR205HG-1, 0.8782 vs. 1.219, P=0.014) and the same trend was also observed in β-catenin

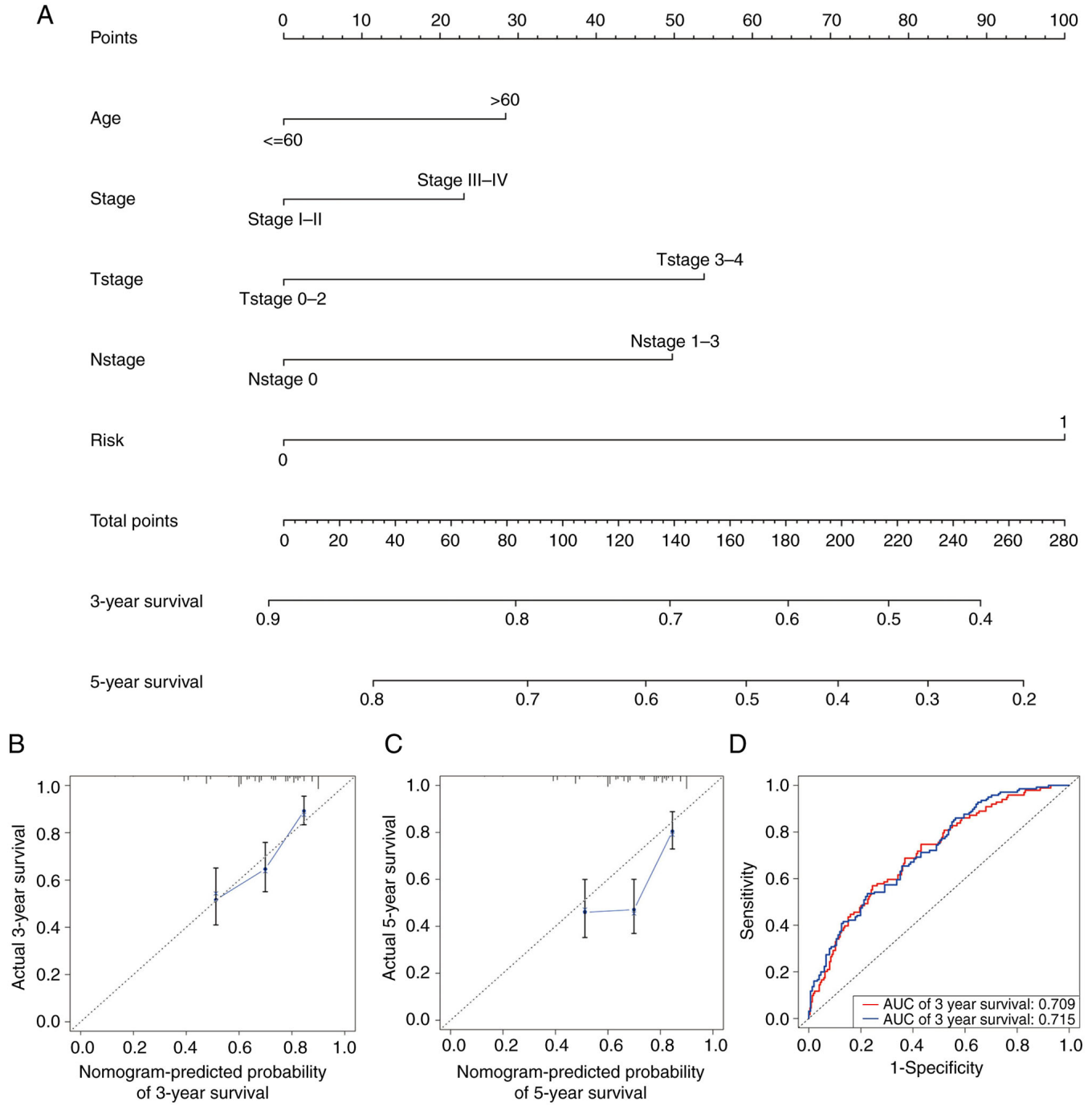

Figure 5. Construction and validation of the prognostic nomogram. (A) Construction of the nomogram was based on traditional clinical variables and the risk score. (B and C) Calibration plot for the internal validation of the nomogram at 3 and 5 years. (D) Time-dependent receiver operating characteristic curves indicating the area under the curve of the nomogram.

(p/t, NC. vs. si-MIR205HG-1, 0.4397 vs. 1.262, P=0.002). Therefore, these results indicated that silencing MIR205HG could partly inhibit the proliferation abilities of melanoma cells through the Wnt/β-catenin signalling pathway.

Discussion

The incidence of melanoma has increased rapidly over the last 50 years worldwide (20). Surgical excision and molecular targeted drugs, which improve the OS and progression-free survival of patients, are the main treatment options for cutaneous melanoma (21). Insufficient understanding of melanoma molecular markers poses a hindrance to melanoma diagnosis and treatment. Therefore, identifying sensitive and specific biomarkers and understanding the mechanisms underlying melanoma development are required to improve the survival rate of patients with melanoma.

Functioning differently in comparison with protein coding sequences, lncRNAs serve an important role in regulating gene expression, which affects chromatin modification, as well as RNA splicing and protein activity. Emerging evidence suggests that lncRNAs could have an effect on the occurrence,

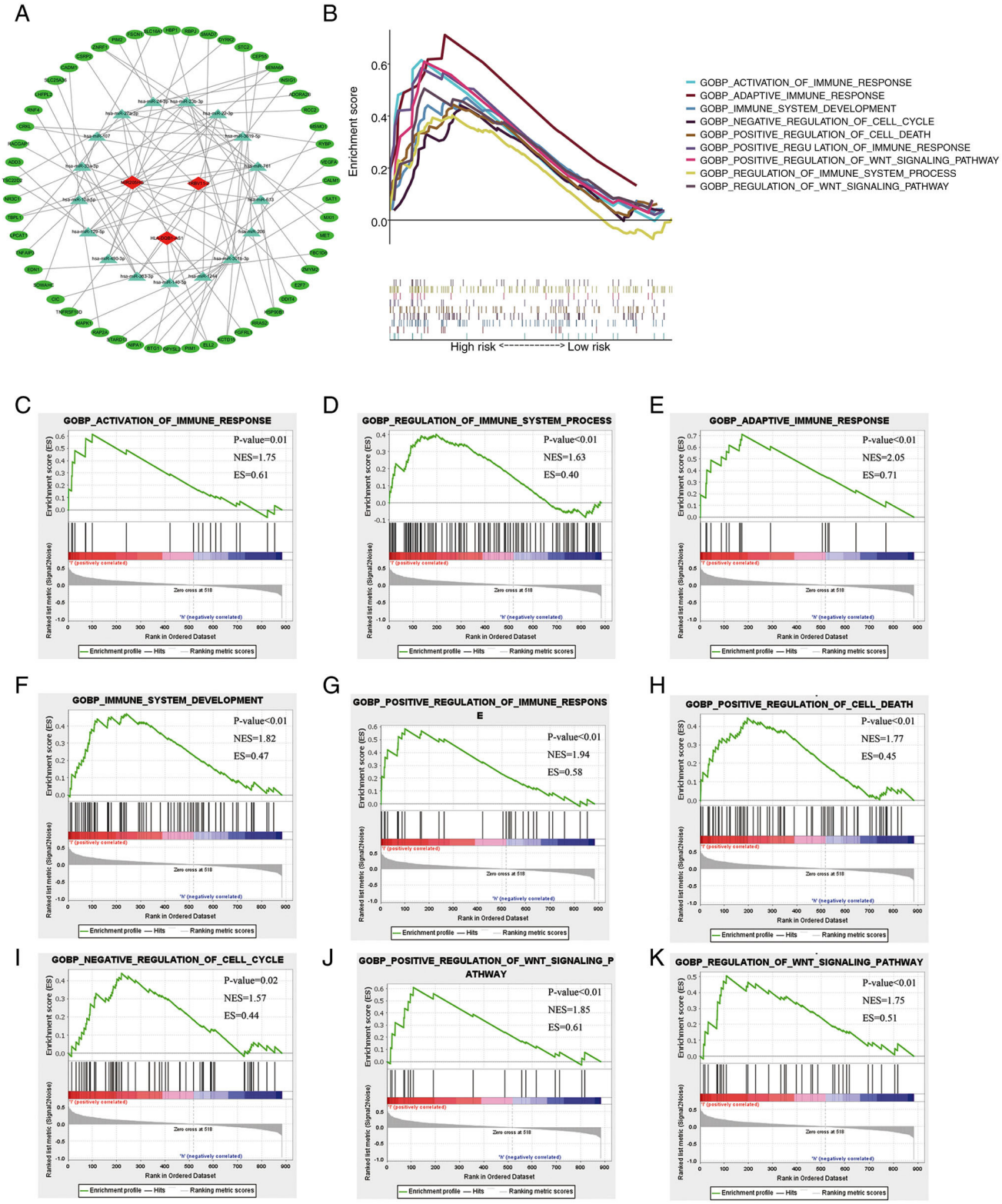

Figure 6. Co-expression RNA regulation network construction and functional enrichment analysis. (A) Construction of a hypoxia-related competing endogenous RNA regulation network based on predicted microRNAs and hypoxia-related mRNAs. (B-K) Gene Ontology-Biological Process gene sets enriched in the high-risk group, including activation of immune response (NES=1.75; P=0.012), regulation of immune system process (NES=1.63; P=0.002), adaptive immune response (NES=2.05; P<0.001), development of immune system (NES=1.82; P<0.001), positive regulation of immune response (NES=1.94; P<0.001), positive regulation of cell death (NES=1.77; P=0.002), negative regulation of cell cycle (NES=1.57; P=0.028), positive regulation of Wnt signalling pathway (NES=1.85; P<0.001) and regulation of Wnt signalling pathway (NES=1.75; P=0.004). NES, normalized enrichment score.

development, prognosis and chemotherapy resistance of tumour cells. Recent studies have reported that lncRNAs, as novel biomarkers, could be used to predict cancer prognosis (22,23). lncRNAs have been reported to be involved in melanoma development by regulating the hypoxia pathway (23,24). Due to consistent overexpression of HOX transcript antisense RNA

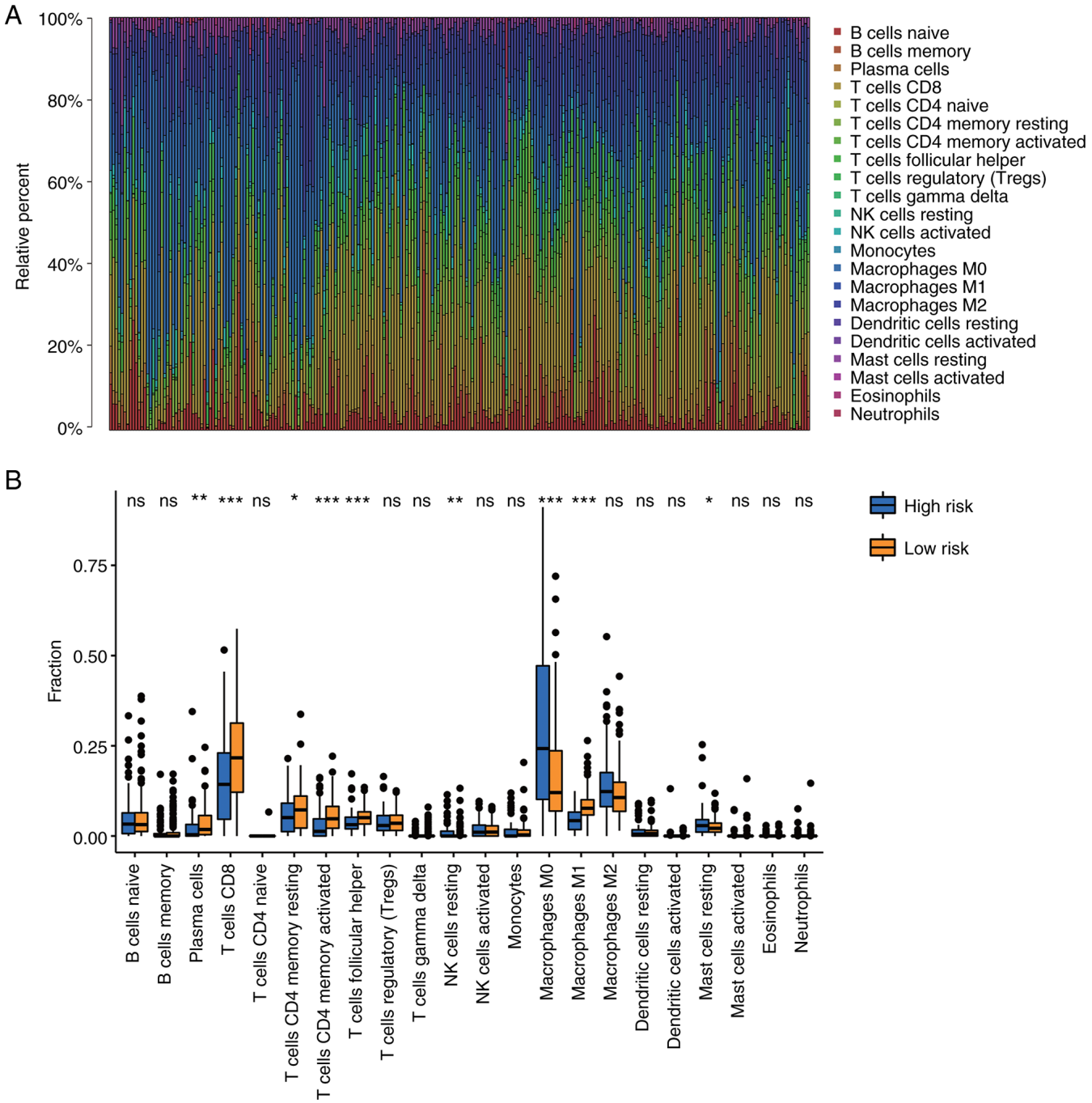

Figure 7. Melanoma is associated with a variety of TIICs. (A) Related percentage of 22 types of TIICs calculated by the CIBERSORT algorithm shown in a bar plot. (B) Differences in infiltration levels of TIICs between the high- and low-risk groups based on the expression of 7 hypoxia-related long non-coding RNAs (unpaired Student's t-test). *P<0.05, **P<0.01 and ***P<0.001. TIICs, tumour-infiltrating immune cells.

(*HOTAIR*), the incidence of lymph node metastasis has been increased compared with primary lesions. However, *HOTAIR* knockdown suppresses the motility and invasion of melanoma cells *in vitro* (25). Aberrant metastasis associated lung adenocarcinoma transcript 1 (*MALAT1*) upregulation promotes melanoma metastasis by stimulating cell migration and de-suppressing miR-140-mediated snail family transcriptional repressor 2 and ADAM metallopeptidase domain 10 inhibition, suggesting that *MALAT1* serves as an oncogenic lncRNA in the development of melanoma (26). BRAF-activated non-protein coding RNA knockout markedly reduces the proliferation of melanoma cells via the MAPK signalling pathway (27), which may act as a prognostic predictor and possible drug target. FGD5 antisense RNA 1 could promote the prognosis in patients with melanoma (28). Furthermore, several lncRNAs, such as antisense RNA in the INK4 locus, SPRY-IT1, Llme23, urothelial cancer associated 1, SRA-like non-coding RNA and survival associated mitochondrial melanoma specific oncogenic non-coding RNA, have been demonstrated to be differentially expressed in patients with melanoma, and to serve a role as potent melanoma progression and metastasis regulators (29). Although recent studies have illustrated the mechanism of melanoma development, the involvement of regulatory lncRNAs in melanoma prognosis under hypoxic conditions remains unclear.

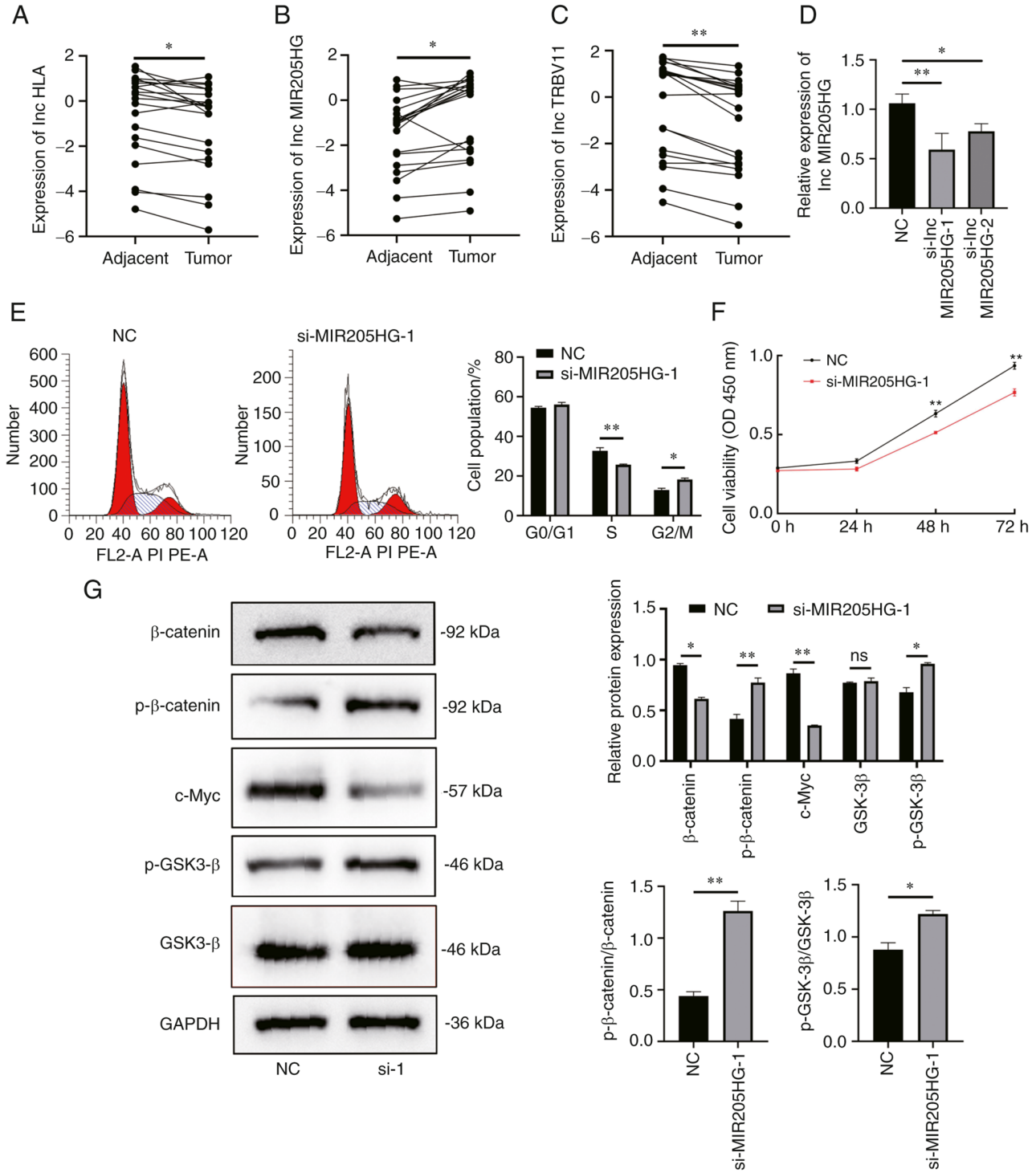

Figure 8. Silencing of MIR205HG inhibits proliferation of melanoma via the canonical Wnt/β-catenin signaling pathway. (A-C) RT-qPCR to detect the expression levels of HLA-DQB1-AS1, MIR205HG-1 and TRBV11-2 in melanoma or paired tissues from 20 patients (Paired Student's t-test; *P<0.05 and **P<0.01). (D) RT-qPCR to detect the relative silencing levels of lncMIR205HG (Data are presented as the mean ± SD; n=3; one-way ANOVA and Dunnett's test; *P<0.05 and **P<0.01). (E) Flow cytometric analysis of the cell cycle distribution in A375 cells after transfection with NC or MIR205HG siRNA. The percentages of cells in G_0/G_1, S and G_2/M phase are shown in the bar graph (n=3; unpaired Student's t-test; *P<0.05 and **P<0.01). (F) Proliferation of A375 cells transfected with NC or si-MIR205HG-1 was assessed using a Cell Counting Kit-8 assay (n=3; one-way ANOVA and Dunnett's test; **P<0.01). (G) β-catenin, p-β-catenin, c-Myc, GSK3-β and p-GSK3-β levels in A375 cells transfected with siRNAs determined by western blotting, ratio of phosphorylated protein to total protein (p/t, phosphorylated/total) about GSK3-β and β-catenin were calculated (n=3; unpaired Student's t-test; *P<0.05 and **P<0.01). MIR205HG, MIR205 host gene; NC, negative control; p-, phosphorylated; RT-qPCR, reverse transcription-quantitative PCR; siRNA/si, small interfering RNA; ns, non-significant.

LncRNAs can modify the regulatory effect of miRNAs on mRNAs (30). Additionally, miRNAs can regulate translation and stability of mRNAs by controlling cellular processes, such as differentiation, apoptosis and migration. In cancer, miRNAs serve an important role in controlling metastasis, invasion and proliferation (31). Zhang *et al* (32) revealed that miR431 can silence DAB2 interacting protein, which is a Ras GTPase activating protein tumor suppressor, to activate Ras/Erk and

promote metastasis of pancreatic neuroendocrine tumors. Feng *et al* (33) revealed that the upregulation of miR-409-3p and Kruppel like factor 17 could inhibit the invasion and migration of gastric cancer cells. In the present study, three lncRNAs from the 7-hypoxia-related-lncRNA signature were further investigated, and these may serve essential roles in the prognosis of patients with melanoma by interacting with the 17 miRNAs and 54 mRNAs predicted. But the potential role of these crucial miRNAs that effect on the prognosis of melanoma remains unknown. Previous studies proved that miRNAs could regulate the biological process of cancer cells through Ras GTPase activity, pErk or EMT process (34,35). In order to render the present study more complete, close attention shall be addressed on how our 7 hypoxia-related-lncRNA affects Ras GTPase activity, as well as the relationship between our signature and pErk and EMT markers.

The present study was based on data downloaded from TCGA database, which contains complete clinical and survival data of patients with melanoma. In the present study, a 7-hypoxia-related-lncRNA signature was constructed, and this included one unfavourable and six favourable lncRNAs as prognostic factors for melanoma. Certain of the lncRNAs have been previously reported to influence tumour prognosis (36). However, there remains a lack of focus on hypoxia-related lncRNAs in melanoma. It has been reported that abnormal HLA expression may influence cytotoxic T lymphocyte and NK cell responses in uveal melanoma (37). According to a study by Serana *et al* (38), TRBV contributes to the promotion of the antitumour T-cell responses in patients with melanoma. Due to its association with multiple tumour-related pathways, MIR205HG-1 was also investigated, particularly in epidermis development and the immune response (39,40). The USP30-mediated stabilisation of dynamin-related protein 1 has been reported to serve a critical role in the development of hepatocellular carcinoma (41). As Lv *et al* (42) reported, a prognostic model based on the 7 lncRNAs, including AL365361, could effectively predict early recurrence after surgical resection of hepatocellular carcinoma. AC022706.1 has also been investigated as a useful biomarker for promoting antitumour immunity and the immunotherapy response in gastric cancers (43). In the present study, a signature of prognosis-related lncRNAs in patients with melanoma was successfully constructed, which was demonstrated to be associated with melanoma progression. The internal validation also demonstrated the accuracy of the present signature. Univariate and multivariate Cox regression analyses demonstrated that the present signature could act as an independent predictor for prognosis prediction of patients with melanoma. Time-dependent ROC curve analysis suggested that the present risk model had the best sensitivity and specificity compared with three other clinicopathological parameters. A novel nomogram based on several crucial clinical features and the present risk score was successfully constructed and validated. These results suggested that the present risk model could be an independent predictor of the survival period in patients with melanoma.

Based on the prediction of different databases and hypoxia-related mRNAs, a co-expression RNA network, including 17 miRNAs and 54 mRNAs, was constructed. Using GSEA, it was revealed that the gene sets enriched in the high-risk group included the activation of immune response, regulation of immune system process, adaptive immune response, development of immune system, negative regulation of cell cycle, positive regulation of cell death, positive regulation of immune response, positive regulation of the Wnt signalling pathway and regulation of the Wnt signalling pathway. Immunotherapy is an important mean of systemic treatment of melanoma, which could improve the prognosis of melanoma, and thus, the present study investigated the relationship between the present risk model and TIICs. The results demonstrated that M0 macrophages, resting mast cells, plasma cells, $CD8^+$ T cells, resting memory $CD4^+$ T cells, activated memory $CD4^+$ T cells, follicular helper T cells, NK cells and M1 macrophages exhibited markedly different infiltration patterns in melanoma. The present results suggested that the 7-hypoxia-related-lncRNA signature could partly reflect the immune infiltration level of melanoma and provide valuable information for immunotherapy.

To validate the prediction of the present signature, the expression levels of HLA, MIR205HG and TRBV11 were detected in 20 clinical samples. The results demonstrated high expression levels of MIR205HG and low expression levels of HLA and TRBV11 in melanoma tissues. The increased MIR205HG expression in melanoma tissues attracted our attention. To investigate the relationship between poor prognosis and aberrant MIR205HG expression, siRNA was used to silence its expression, resulting in suppressed proliferation of melanoma A375 cells. These results suggested that MIR205HG is a target that can promote melanoma proliferation. The dysregulation of cell cycle control is an obstacle to the suppression of melanoma growth (44). Agents targeting the G_1/S and G_2/M checkpoints have shown promising preclinical activity in patients with melanoma (45,46). Because si-MIR205HG-1 suppressed proliferation in A375 cells, cell cycle arrest was investigated using flow cytometry in si-MIR205HG-1 cells. Cell aggregation that decreased at the S phase but increased at the G_2/M phase was observed after treatment with si-MIR205HG-1. These results demonstrated that silencing MIR205HG may inhibit melanoma cell proliferation at the G_2/M phase, which could partly explain the relationship between the present risk model based on the expression of 7 hypoxia-related lncRNAs and poor prognosis of patients with melanoma.

The aberrant activation of canonical Wnt/β-catenin signalling is observed in multiple malignant tumours and is recognised as an attractive therapeutic target for molecular drugs (47). It has been reported that Wnt serves a crucial role in tumorigenesis and malignancy, which contributes to tumour proliferation and differentiation, survival, stress response and resistance (48). To elucidate the molecular mechanisms of the effect of si-MIR205HG-1 on cell proliferation, regulatory proteins of the Wnt/β-catenin signalling pathway were examined in A375 cells using western blot analysis. Increased p-GSK3-β levels in A375 cells decreased β-catenin and c-Myc expression, resulting in low si-MIR205HG-1 expression. These results demonstrated that the silencing of MIR205HG-1 inhibited the proliferation of melanoma via the canonical Wnt/β-catenin signalling pathway. LncRNA can influence tumor cell migration and invasion. Chen *et al* (16) revealed that NORAD may play critical roles in tumorigenesis and progression of malignant melanoma by regulating

of the MIR205-EGLN2 pathway. Xu *et al* (49) revealed that lncRNA CRNDE can promote the migration and invasion of melanoma by sponging MIR205 and releasing CCL18. And in the present study, it was primarily identified that the overexpression of MIR205HG could inhibit the proliferation of melanoma cells through the canonical Wnt/β-catenin signalling pathway. In order to render the present study more thorough, it will be investigated in future studies how the dose of our 7 hypoxia-related-lncRNA influences melanoma by cell migration and invasion.

The present study has several limitations. The present prognostic model should be further validated using a larger clinical sample size with adequate follow-up duration. In addition, the underlying mechanisms of how these 7 lncRNAs or some of them influence the proliferation of melanoma should be more comprehensively investigated. The detailed mechanisms of how MIR205HG inhibits the proliferation of melanoma cells via the canonical Wnt/β-catenin signalling pathway require more exploration and validation. Furthermore, the present study lacks animal experiments, which will be verified in further exploration.

At present, there were kinds of lncRNA signatures used to predict the prognosis of melanoma. Although hypoxia is an important circumstance for melanoma cells surviving, the study focused on hypoxia-related-lncRNA signature has not been reported yet. Moreover, MIR205HG played an important role in influencing the pluripotency, proliferation (50), and dissemination of malignant melanoma (51). Nevertheless, few of them paid attention to investigate and verify that MIR205HG could be a prognostic biomarker and an actionable target for inhibiting proliferation of melanoma.

In conclusion, a novel 7-hypoxia-related-lncRNA signature was preliminarily constructed and validated to promote the prognostic prediction of patients with melanoma. Based on this risk model, a nomogram and ceRNA network were successfully constructed to provide a new sight of investigating the underlying molecular mechanism of melanoma. Among these lncRNAs, supressing the overexpression of MIR205HG inhibited the proliferation of melanoma cells via the canonical Wnt/β-catenin signalling pathway, which could partly explain the relationship between the present risk model and poor prognosis of patients with melanoma.

Acknowledgements

Not applicable.

Funding

No funding was received.

Availability of data and materials

The datasets used and/or analyzed during the current study are available from the corresponding author on reasonable request.

Authors' contributions

YL and AJC designed and implemented experiments. THL and HGZ collected data and performed statistical analysis. YL and THL helped perform the analysis with constructive discussions and revised the manuscript carefully. All authors read and approved the final manuscript. YL and AJC confirm the authenticity of all the raw data.

Ethics approval and consent to participate

This article meets the requirements of TCGA and other websites for publication and does not contain any studies involving animals performed by any of the authors. The study was approved (approval no. 2021-487) by the Ethics Committee of the First Affiliated Hospital of Chongqing Medical University. All individuals provided written informed consent for the use of their samples for clinical research.

Patient consent for publication

Not applicable.

Competing interests

The authors declare that they have no competing interests.

References

1. Leonardi GC, Falzone L, Salemi R, Zanghì A, Spandidos DA, Mccubrey JA, Candido S and Libra M: Cutaneous melanoma: From pathogenesis to therapy (Review). Int J Oncol 52: 1071-1080, 2018.
2. Davey MG, Miller N and McInerney NM: A review of epidemiology and cancer biology of malignant melanoma. Cureus 13: e15087, 2021.
3. Carr S, Smith C and Wernberg J: Epidemiology and risk factors of melanoma. Surg Clin North Am 100: 1-12, 2020.
4. Lu X and Kang Y: Hypoxia and hypoxia-inducible factors: Master regulators of metastasis. Clin Cancer Res 16: 5928-5935, 2010.
5. Liu Y, Ciotti GE and Eisinger-Mathason TSK: Hypoxia and the tumor secretome. Adv Exp Med Biol 1136: 57-69, 2019.
6. Graham K and Unger E: Overcoming tumor hypoxia as a barrier to radiotherapy, chemotherapy and immunotherapy in cancer treatment. Int J Nanomedicine 13: 6049-6058, 2018.
7. Jing X, Yang F, Shao C, Wei K, Xie M, Shen H and Shu Y: Role of hypoxia in cancer therapy by regulating the tumor microenvironment. Mol Cancer 18: 157, 2019.
8. Qiu H, Chen F and Chen M: MicroRNA-138 negatively regulates the hypoxia-inducible factor 1α to suppress melanoma growth and metastasis. Biol Open 8: bio042937, 2019.
9. Dong L, You S, Zhang Q, Osuka S, Devi NS, Kaluz S, Ferguson JH, Yang H, Chen G, Wang B, *et al*: Arylsulfonamide 64B inhibits hypoxia/HIF-induced expression of c-Met and CXCR4 and reduces primary tumor growth and metastasis of uveal melanoma. Clin Cancer Res 25: 2206-2218, 2019.
10. Quinn JJ and Chang HY: Unique features of long non-coding RNA biogenesis and function. Nat Rev Genet 17: 47-62, 2016.
11. Jarroux J, Morillon A and Pinskaya M: History, discovery, and classification of lncRNAs. Adv Exp Med Biol 1008: 1-46, 2017.
12. Liu M, Zhong J, Zeng Z, Huang K, Ye Z, Deng S, Chen H, Xu F, Li Q and Zhao G: Hypoxia-induced feedback of HIF-1α and lncRNA-CF129 contributes to pancreatic cancer progression through stabilization of p53 protein. Theranostics 9: 4795-4810, 2019.
13. Piao HY, Liu Y, Kang Y, Wang Y, Meng XY, Yang D and Zhang J: Hypoxia associated lncRNA HYPAL promotes proliferation of gastric cancer as ceRNA by sponging miR-431-5p to upregulate CDK14. Gastric Cancer 25: 44-63, 2022.
14. Yu Z, Wang Y, Deng J, Liu D, Zhang L, Shao H, Wang Z, Zhu W, Zhao C and Ke Q: Long non-coding RNA COL4A2-AS1 facilitates cell proliferation and glycolysis of colorectal cancer cells via miR-20b-5p/hypoxia inducible factor 1 alpha subunit axis. Bioengineered 12: 6251-6263, 2021.

15. Liu Y, He D, Xiao M, Zhu Y, Zhou J and Cao K: Long noncoding RNA LINC00518 induces radioresistance by regulating glycolysis through an miR-33a-3p/HIF-1α negative feedback loop in melanoma. Cell Death Dis 12: 245, 2021.
16. Chen Y, Cao K, Li J, Wang A, Sun L, Tang J, Xiong W, Zhou X, Chen X, Zhou J and Liu Y: Overexpression of long non-coding RNA NORAD promotes invasion and migration in malignant melanoma via regulating the MIR-205-EGLN2 pathway. Cancer Med 8: 1744-1754, 2019.
17. Wu L, Liu G, He YW, Chen R and Wu ZY: Identification of a pyroptosis-associated long non-coding RNA signature for predicting the immune status and prognosis in skin cutaneous melanoma. Eur Rev Med Pharmacol Sci 25: 5597-5609, 2021.
18. Chen H, Pan Y, Jin X and Chen G: Identification of a four hypoxia-associated long non-coding RNA signature and establishment of a nomogram predicting prognosis of clear cell renal cell carcinoma. Front Oncol 11: 713346, 2021.
19. Livak KJ and Schmittgen TD: Analysis of relative gene expression data using real-time quantitative PCR and the 2(-Delta Delta C(T)) method. Methods 25: 402-408, 2001.
20. Raimondi S, Suppa M and Gandini S: Melanoma epidemiology and sun exposure. Acta Derm Venereol 100: adv00136, 2020.
21. Pavri SN, Clune J, Ariyan S and Narayan D: Narayan, malignant melanoma: Beyond the basics. Plast Reconstr Surg 138: 330e-340e, 2016.
22. Zhang H, Qin C, Liu HW, Guo X and Gan H: An effective hypoxia-related long non-coding RNAs assessment model for prognosis of clear cell renal carcinoma. Front Oncol 11: 616722, 2021.
23. Gong PJ, Shao YC, Huang SR, Zeng YF, Yuan XN, Xu JJ, Yin WN, Wei L and Zhang JW: Hypoxia-associated prognostic markers and competing endogenous RNA Co-expression networks in breast cancer. Front Oncol 10: 579868, 2020.
24. Chi Y, Wang D, Wang J, Yu W and Yang J: Long non-coding RNA in the pathogenesis of cancers. Cells 8: 1015, 2019.
25. Zhang J, Liu H, Zhang W, Li Y, Fan Z, Jiang H and Luo J: Identification of lncRNA-mRNA regulatory module to explore the pathogenesis and prognosis of melanoma. Front Cell Dev Biol 8: 615671, 2020.
26. Sun L, Sun P, Zhou QY, Gao X and Han Q: Long noncoding RNA MALAT1 promotes uveal melanoma cell growth and invasion by silencing of miR-140. Am J Transl Res 8: 3939-3946, 2016.
27. Yu X, Zheng H, Chan MT and Wu WKK: BANCR: A cancer-related long non-coding RNA. Am J Cancer Res 7: 1779-1787, 2017.
28. Gao Y, Zhu H and Mao Q: Expression of lncRNA FGD5-AS1 correlates with poor prognosis in melanoma patients. J Gene Med 22: e3278, 2020.
29. Yu X, Zheng H, Tse G, Chan MT and Wu WK: Long non-coding RNAs in melanoma. Cell Prolif 51: e12457, 2018.
30. Karagkouni D, Karavangeli A, Paraskevopoulou MD and Hatzigeorgiou AG: Characterizing miRNA-lncRNA interplay. Methods Mol Biol 2372: 243-262, 2021.
31. Lai X, Eberhardt M, Schmitz U and Vera J: Systems biology-based investigation of cooperating microRNAs as monotherapy or adjuvant therapy in cancer. Nucleic Acids Res 47: 7753-7766, 2019.
32. Zhang T, Choi S, Zhang T, Chen Z, Chi Y, Huang S, Xiang JZ and Du YN: miR-431 promotes metastasis of pancreatic neuroendocrine tumors by targeting DAB2 interacting protein, a ras GTPase activating protein tumor suppressor. Am J Pathol 190: 689-701, 2020.
33. Feng J, Li K, Liu G, Feng Y, Shi H and Zhang X: Precision hyperthermia-induced miRNA-409-3p upregulation inhibits migration, invasion, and EMT of gastric cancer cells by targeting KLF17. Biochem Biophys Res Commun 549: 113-119, 2021.
34. Salminen A, Kaarniranta K, Kauppinen A, Ojala J, Haapasalo A, Soininen H and Hiltunen M: Impaired autophagy and APP processing in Alzheimer's disease: The potential role of Beclin 1 interactome. Prog Neurobiol 106-107: 33-54, 2013.
35. Su J, Morgani SM, David CJ, Wang Q, Er EE, Huang YH, Basnet H, Zou Y, Shu W, Soni RK, *et al*: TGF-β orchestrates fibrogenic and developmental EMTs via the RAS effector RREB1. Nature 577: 566-571, 2020.
36. Zhang B, Tang B, Gao J, Li J, Kong L and Qin L: A hypoxia-related signature for clinically predicting diagnosis, prognosis and immune microenvironment of hepatocellular carcinoma patients. J Transl Med 18: 342, 2020.
37. Souri Z, Wierenga APA, Mulder A, Jochemsen AG and Jager MJ: HLA expression in uveal melanoma: An indicator of malignancy and a modifiable immunological target. Cancers (Basel) 11: 1132, 2019.
38. Serana F, Sottini A, Caimi L, Palermo B, Natali PG, Nisticò P and Imberti L: Identification of a public CDR3 motif and a biased utilization of T-cell receptor V beta and J beta chains in HLA-A2/Melan-A-specific T-cell clonotypes of melanoma patients. J Transl Med 7: 21, 2009.
39. Guo J, Gan Q, Gan C, Zhang X, Ma X and Dong M: LncRNA MIR205HG regulates melanomagenesis via the miR-299-3p/VEGFA axis. Aging (Albany NY) 13: 5297-5311, 2021.
40. Liu N, Liu Z, Liu X and Chen H: Comprehensive analysis of a competing endogenous RNA network identifies seven-lncRNA signature as a prognostic biomarker for melanoma. Front Oncol 9: 935, 2019.
41. Gu L, Zhu Y, Lin X, Li Y, Cui K, Prochownik EV and Li Y: Amplification of glyceronephosphate O-acyltransferase and recruitment of USP30 stabilize DRP1 to promote hepatocarcinogenesis. Cancer Res 78: 5808-5819, 2018.
42. Lv Y, Wei W, Huang Z, Chen Z, Fang Y, Pan L, Han X and Xu Z: Long non-coding RNA expression profile can predict early recurrence in hepatocellular carcinoma after curative resection. Hepatol Res 48: 1140-1148, 2018.
43. He Y and Wang X: Identification of molecular features correlating with tumor immunity in gastric cancer by multi-omics data analysis. Ann Transl Med 8: 1050, 2020.
44. Xu W and McArthur G: Cell cycle regulation and melanoma. Curr Oncol Rep 18: 34, 2016.
45. Barnaba N and LaRocque JR: Targeting cell cycle regulation via the G2-M checkpoint for synthetic lethality in melanoma. Cell Cycle 20: 1041-1051, 2021.
46. Afrang N and Honardoost M: Cell cycle regulatory markers in melanoma: New strategies in diagnosis and treatment. Med J Islam Repub Iran 33: 96, 2019.
47. Nishiya N: Screening for chemical suppressors of the Wnt/β-catenin signaling pathway. Yakugaku Zasshi 137: 133-136, 2017 (In Japanese).
48. Xue G, Romano E, Massi D and Mandalà M: Wnt/β-catenin signaling in melanoma: Preclinical rationale and novel therapeutic insights. Cancer Treat Rev 49: 1-12, 2016.
49. Xu L, Zhang Y, Zhao Z, Chen Z, Wang Z, Xu S, Zhang X, Liu T and Yu S: The long non-coding RNA CRNDE competed endogenously with miR-205 to promote proliferation and metastasis of melanoma cells by targeting CCL18. Cell Cycle 17: 2296-2308, 2018.
50. Sahranavardfard P, Madjd Z, Emami Razavi AN, Ghanadan AR, Firouzi J, Khosravani P, Ghavami S, Ebrahimie E and Ebrahimi M: An integrative analysis of the Micro-RNAs contributing in stemness, metastasis and B-Raf pathways in malignant melanoma and melanoma stem cell. Cell J 23: 261-272, 2021.
51. Sánchez-Sendra B, Serna E, Navarro L, González-Muñoz JF, Portero J, Ramos A, Murgui A and Monteagudo C: Transcriptomic identification of miR-205 target genes potentially involved in metastasis and survival of cutaneous malignant melanoma. Sci Rep 10: 4771, 2020.

This work is licensed under a Creative Commons Attribution-NonCommercial-NoDerivatives 4.0 International (CC BY-NC-ND 4.0) License.